ISSN 0022-4766, Journal of Structural Chemistry, 2023, Vol. 64, No. 3, pp. 337-346. © Pleiades Publishing, Ltd., 2023.
Russian Text © The Author(s), 2023, published in Zhurnal Strukturnoi Khimii, 2023, Vol. 64, No. 3, 106824.

INFLUENCE OF MAGNETIC FIELD ON THE STRUCTURE AND SENSOR PROPERTIES OF THIN TITANYL PHTHALOCYANINE LAYERS

S. E. Dyusenova[1,2], D. D. Klyamer[1], A. S. Sukhikh[1,2]*, I. M. Shchudlo[2,3], S. Y. Taskaev[2,3], T. V. Basova[1], and S. A. Gromilov[1,2]

We report a study of the effect of magnetic field on the structural organization and sensory properties of thin titanyl phthalocyanine (TiOPc) layers deposited by vacuum thermal evaporation. It is shown that magnetic field (directed perpendicular to the substrate surface) does not affect the phase composition of the layers which are represented by II-triclinic and I-monoclinic crystal modifications in both cases. The crystallites of both phases demonstrate preferential orientations, the angles between molecular planes and the substrate are 62.53° and 5.30°, respectively. The 2D GIXD study shows that magnetic field significantly improves the crystallinity of obtained thin layers; the conductivity increases by ~10 times, but the sensory response to ammonia does not change. Irradiating the layer obtained in magnetic field by fast neutrons (fluence $3 \cdot 10^{14}$ cm^{-2}) decreases the conductivity by two orders of magnitude. This effect is not observed in the parallel experiment without magnetic field.

DOI: 10.1134/S0022476623030010

Keywords: metal phthalocyanines, film, powder XRD, 2D GIXD, structural organization of films, conductivity, sensory response, fast neutrons.

INTRODUCTION

Among numerous organic semiconductors, metal phthalocyanines (MPc) are particularly interesting due to their high thermal and chemical stability and unique electronic properties. The ability of MPc to sublimate in vacuum allows preparing thin homogeneous highly oriented polycrystalline layers by vacuum thermal evaporation, which is increasingly often used not only in the production of field-effect transistors, solar cells, diodes, etc. [1], but also as active layers of chemical sensors [2].

The structure and orientation of molecules in ordered MPc layers are most important for their application in electronic devices. Thus, the authors of [1] state that most efficient charge transfer in organic field-effect transistors is achieved when molecules are packed along the direction of current in the conducting channel. An important feature of MPc layers is the absence of strong interactions between terminal molecules deposited on a smooth substrate surface.

[1]Nikolaev Institute of Inorganic Chemistry, Siberian Branch, Russian Academy of Sciences, Novosibirsk, Russia; *a_sukhikh@niic.nsc.ru. [2]Novosibirsk State University, Novosibirsk, Russia. [3]Budker Institute of Nuclear Physics, Siberian Branch, Russian Academy of Sciences, Novosibirsk, Russia. Original article submitted November 22, 2022; revised January 13, 2023; accepted January 16, 2023.

Consequently, the choice of deposition conditions can significantly affect the growth process and structural organization of layers. In addition to traditional methods of affecting the orientation of molecules in MPc layers (temperature parameters, growth rate, substrate material) [3-5], the attention of researchers was relatively recently attracted by the impact of external electrical [6-8] and magnetic fields [9, 10]. For example, it was shown in [6] that electric field affects the orientation and phase composition of unsubstituted phthalocyanine (H_2Pc) layers. Also, layers deposited under the action of electric field can have enhanced conductivity, as it was demonstrated in [8] on the example of CuPc layers. The authors of [7] studied the influence of electric field on the structural organization and morphology of the surface of TiOPc layers deposited on a sapphire substrate. The authors showed deposition without electric field results in the I-monoclinic TiOPc modification, while electric field directed perpendicular to the substrate plane leads to the formation of the II-triclinic TiOPc modification, and the angle between the plane of the molecule and the substrate diminishes from ~90° to ~60°.

There are much fewer studies of the effect of magnetic field on the structural organization of MPc layers. The influence of magnetic field was described on the example of CuPc in [9]. The deposition was carried out in magnetic field (6 mT) directed perpendicular to the substrate plane. The XRD pattern showed a reflection from the family of crystallographic planes {010} with the interplanar distance $d = 4.0$ Å. The authors concluded that this value is most close to the parameter $b = 3.769$ Å corresponding to the α-modification of CuPc [11]. This means that most of CuPc crystallites are oriented along the b axis, i.e. perpendicular to the substrate plane. However, this conclusion is doubtful, since the interplanar distance d_{010} cannot be larger than parameter b. Moreover, the XRD pattern of CuPc layers obtained by the authors does not correspond to any known crystal modification of CuPc. The problem of conducting reliable phase analysis is also faced in the studies of the layers of TiOPc that has five known polymorphs: II-triclinic [12], I-monoclinic [12], Y-monoclinic [13], IV-triclinic [14], and C-monoclinic [15] (referred to below as II, I, Y, IV, C).

We have not succeeded in finding studies of TiOPc layers prepared in magnetic fields, but there are several reported papers on its structural analog vanadyl phthalocyanine (VOPc). The authors of [10] studied the structure and morphology of thin VOPc layers deposited in an external magnetic field directed perpendicular to the substrate surface. It was shown that magnetic field does not affect the crystallinity and morphology of the surface of layers. The spectral ellipsometry data show that the angle between the molecules and the substrate surface in the layers deposited in a magnetic field decreases from 24° to 3° compared to those deposited under normal conditions. It was shown in [16, 17] that conductivity of VOPc films increases in the presence of magnetic field directed parallel to the substrate surface.

The authors of [10] explained the effect of magnetic field on the structural organization of VOPc layers by assuming that strong magnetic field directed perpendicular to the plane of the diamagnetic MPc molecule containing benzene rings or aromatic heterocycles induces electric current directed perpendicularly within the molecule. In turn, this current creates magnetic dipole with a vector directed opposite to the applied field. As a result, the MPc molecule adopts an unstable high-energy state and is to orient the way that the aromatic rings be parallel to the lines of the applied field. Note also that crystallite formation on the substrate surface is a collective process involving a multitude of molecules.

In the case of non-planar molecules such as VOPc and TiOPc the description of crystallization can be much more difficult due to the inner electric dipole moment of the molecules. It should also be noted that, despite structural similarity, TiOPc molecules are diamagnetic while VOPc molecules are paramagnetic [18]. Therefore, the influence of magnetic field on TiOPc layers can differ significantly from the results obtained for VOPc. The above examples show that magnetic field can be used to control structural organization of thin layers during their growth.

Standard X-ray diffraction analysis in the Bragg–Brentano focusing geometry poorly suits for the analysis of structural organization of highly oriented thin layers, i.e. polycrystalline layers where the absolute majority of crystallites are oriented along a certain crystallographic direction. As a result, the XRD patterns of such samples are uninformative and represent the orders of reflections from one family of crystallographic planes. TiOPc has five known polymorphs; therefore, powder XRD analysis of this compound is difficult, since the observed diffraction peaks can be assigned to two or more phases. This limitation can be overcome by using 2D grazing incidence X-ray diffraction (2D GIXD). Recording in the 2D GIXD geometry implies a single-crystal diffractometer with a phthalocyanine sample attached to the instrument by a special

adapter. A narrow collimated X-ray beam falls onto the sample under a small (0-1°) angle, and the resulting diffraction pattern is recorded by a 2D detector. For the 2D GIXD geometry, a sample's preferential orientation is a positive quality, since the diffraction pattern does not show diffraction rings or arcs but isolated well-localized diffraction spots. The use of 2D GIXD geometry is described in more detail in [19].

The purpose of this work is to study the crystal structure and morphology of TiOPc thin layers obtained by vacuum thermal evaporation with and without magnetic field. The role of deposition conditions in the adsorption-resistive sensory response of TiOPc layers to ammonia was also studied.

EXPERIMENTAL

Synthesis of TiOPc. TiOPc was synthesized by heating a mixture of phthalonitrile, tetrabutoxytitanium, urea, and octanol in the 4:1:2:5 molar ratio up 160 °C for 6 h under constant stirring. The resulting green thick mixture was washed with ethyl alcohol, dried for 24 hours, and purified twice by gradient sublimation in vacuum ($1 \cdot 10^{-5}$ mmHg) at 420-440 °C. The obtained product was a polycrystalline powder of fine (30×300 μm) needle-shaped dark blue crystals with metallic sheen. The XRD data (Fig. 1) show that the product consists of two TiOPc modifications: II and I. Exact phase ratio was not determined due to pronounced preferential orientation of crystallites in the sample.

Deposition of TiOPc films. TiOPc layers were prepared by vacuum thermal evaporation in a VUP-5M installation under a residual pressure of $1 \cdot 10^{-5}$ mmHg. TiOPc powder was loaded in a Knudsen chamber and heated up to 450 °C. The temperature was controlled with a Termodat-131 thermostat using a K-type thermocouple. The substrates were 10×10×0.1 mm glass plates (optical microscope cover slips) positioned 10 cm above the Knudsen chamber (Fig. 2). The deposition time was 1 h.

The effect of magnetic field on structural organization of films was studied using depositions with and without magnetic field. Magnetic field was created by a cube neodymium magnet (grade N35, 1×1×1 cm, ~0.5 T) applied to the top of the substrate so that the magnetic field was directed perpendicular to the substrate surface (referred to below as the $TiOPc_M$ sample). Note that the magnet employed in the deposition process has a noticeable thermal mass so that it acts as a kind of cooling “radiator” for the substrate and can affect the properties of the resulting layers. To avoid that, we demagnetized

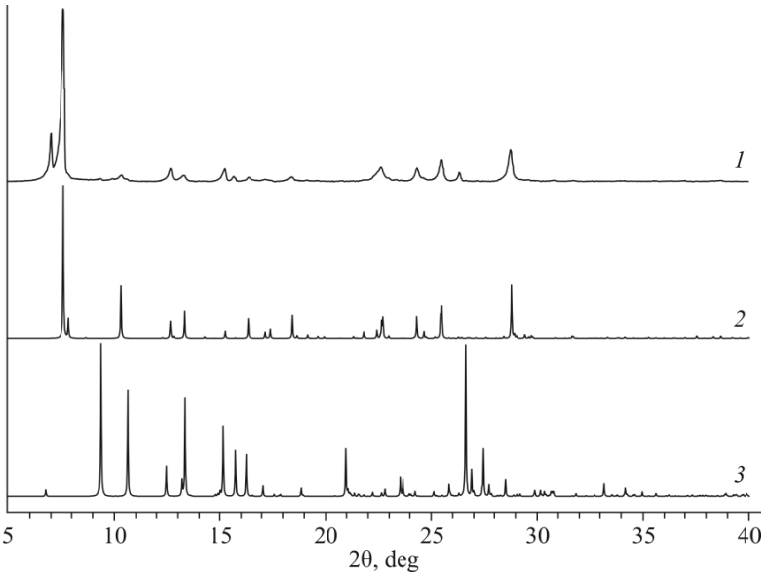

Fig. 1. XRD pattern (Shimadzu XRD-7000, CuK_α radiation, Bragg–Brentano geometry) of the synthesized product (*1*) juxtaposed with theoretical XRD patterns of II-triclinic (*2*) and I-monoclinic (*3*) TiOPc polymorphs.

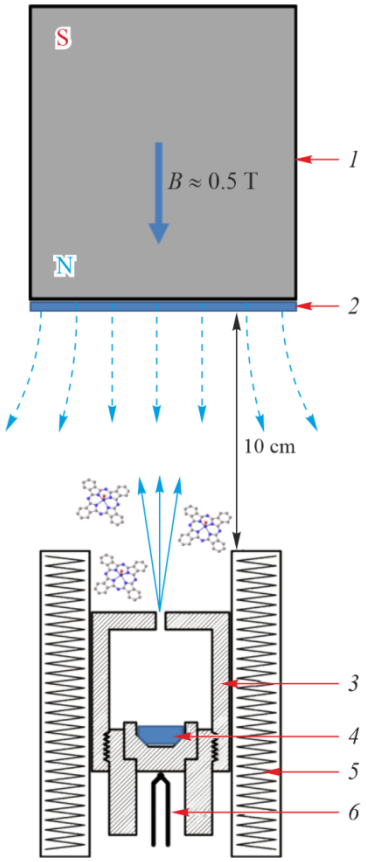

Fig. 2. Setup for the deposition of thin TiOPc layers in magnetic field by vacuum thermal evaporation: neodymium magnet (*1*), substrate (*2*), Knudsen chamber (*3*), TiOPc powder (*4*), heater (*5*), thermocouple (*6*).

a magnet by preheating it above the Curie temperature and applied it to the back side of the substrate of samples prepared without magnetic field (referred to below as the $TiOPc_0$ sample). In total, three pairs of thin films were studied.

X-ray diffraction and atomic force microscopy. Powder diffraction of TiOPc thin layers in Bragg–Brentano focusing geometry was performed on a Shimadzu XRD-7000 powder diffractometer (CuK_α radiation, 40 kV, 30 mA, vertical θ–θ goniometer with a radius of 200 mm, Ni filter, OneSight SSD detector). The measurements were conducted in the 2θ range from 5° to 40° with a scan step of 0.03° and a total acquisition time per point of 120 s. Preferential orientation was reduced by rotating the sample in its proper plane at a speed of 60 rpm. The resulting XRD patterns are shown in Fig. 3.

The 2D GIXD study of TiOPc films was conducted on a Bruker DUO single-crystal diffractometer (Incoatec IμS microfocus tube, CuK_α radiation, APEX II CCD detector with a resolution of 1024×1024, pixel size 60×60 μm). Strips with a width of 2-3 mm were cut from the initial samples and fixed with special adapter in the goniometer head. During the measurements, the detector was positioned perpendicular to the primary beam ($2\theta_D = 0°$) at a distance of 80 mm from the sample. The angle between the incident primary beam and the sample plane was ~0.5°. The total acquisition time for each diffraction pattern was 10 min. the obtained 2D diffraction patterns (Fig. 4, 5) wre processed with the XRD2DScan 4.1.1 program [20].

Surface morphology and thickness of the samples were studied using an NT-MDT NEXT II atomic force microscope (NSU, Youth Laboratory of Functional Diagnostics of Nanoscale Systems, Head P. Geydt) in semi-contact mode

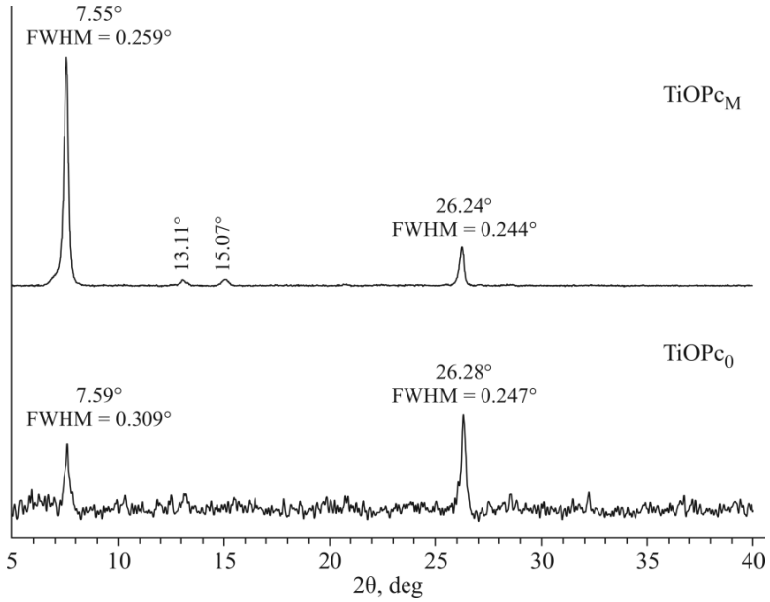

Fig. 3. XRD patterns (Shimadzu XRD-7000, CuK_α radiation, Bragg–Brentano geometry) of TiOPc layers deposited with (TiOPc$_M$) and without (TiOPc$_0$) magnetic field. Intensity of the upper XRD pattern is diminished by 80 times.

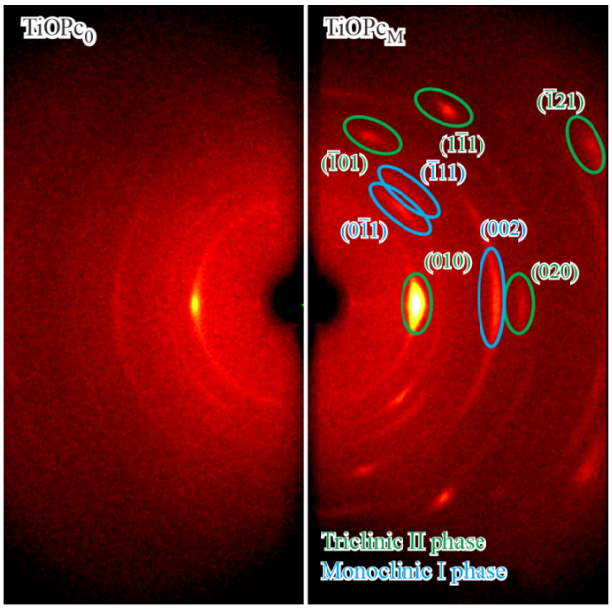

Fig. 4. XRD patterns of TiOPc$_M$ and TiOPc$_0$ films (Bruker DUO, CuK_α radiation, 2D GIXD geometry).

at room temperature. The obtained images were processed using the Gwyddion v.2.61 program [21]. The results are shown in Fig. 6.

Adsorption-resistive sensory response of the films. Adsorption-resistive sensory response of layers to ammonia, TiOPc films (in parallel with the main samples) were deposited on glass substrates with platinum interdigital transducers (IDT, DropSens) separated by a distance of 10 μm. Sensory response measurement is based on the change in the metal phthalocyanine film's resistance as the composition of the gas mixture changes. The resulting samples were placed in a gas flow chamber that was constantly purged with diluent gas (air). Then controlled concentrations of ammonia were supplied to the chamber. The sensory response was measured in the dynamic mode. The analyte gas was supplied into the gas chamber

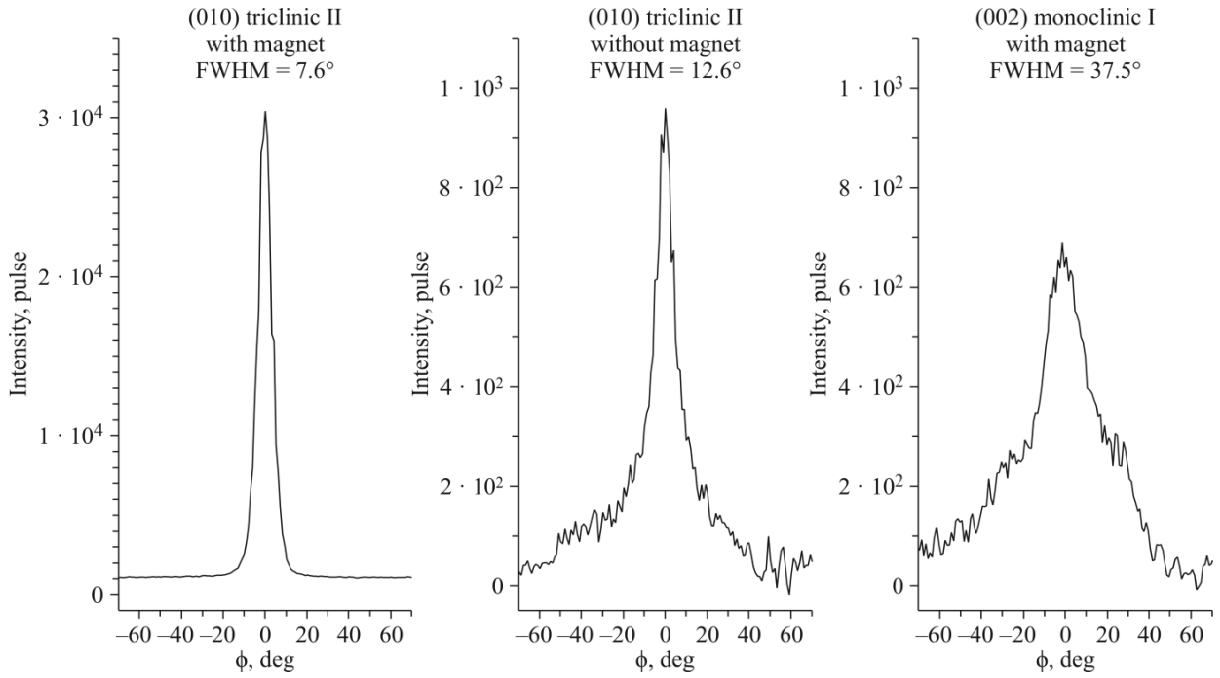

Fig. 5. Azimuthal peak profiles of (010) II-triclinic and (002) I-monoclinic modifications of $TiOPc_M$ and $TiOPc_0$ films.

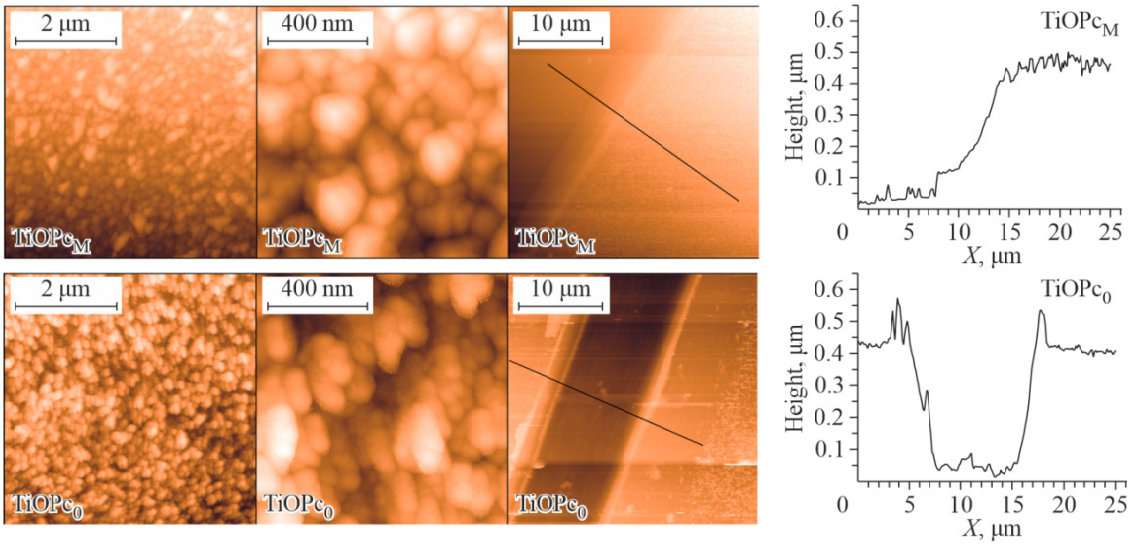

Fig. 6. AFM images and the thickness profile of $TiOPc_M$ and $TiOPc_0$ films.

for 15 s; as a result, the film resistance changed sharply, and the chamber was purged with air until the initial resistance value. The film resistance was measured using a Keithley-236 universal electrometer at a constant voltage of 10 V; adsorption-resistive response of was measured in the range of ammonia concentrations from 10 μm to 50 μm. All experiments were carried out at room temperature.

RESULTS AND DISCUSSION

The XRD pattern of the $TiOPc_M$ film prepared in magnetic field (Fig. 3) shows two pairs of diffraction peaks at 2θ angles of 7.55°/15.07° and 13.11°/26.24°, obviously corresponding to two groups of crystallographic planes. In both groups, the ratio of interplanar distances is 2:1. None of five TiOPc polymorphs explains all these reflections, so the sample most

likely consists of two phases. Formation of a new modification can neither be excluded. The fact that only reflection orders are present indicates strong preferential orientation. The first pair of diffraction peaks can be assigned to modification II (theoretical angular positions of diffraction peaks (010) and (020) are 7.61° and 15.26° 2θ) and to modification IV: peaks (010) and (020) at 7.53° and 15.09° 2θ, respectively. The Y modification with diffraction peaks (100) at 7.39° and (200) at 14.81° 2θ is also possible, even though less probable. The second pair of diffraction peaks most likely belongs to modification I: peak (002) at 13.20° and peak (004) at 26.58° 2θ. Other modifications, namely IV and Y, have diffraction peaks with matching angular positions but with different ratios of their first and second order intensities.

The XRD reflections of the $TiOPc_0$ film are much less (~100 times) intense than those of $TiOPc_M$ (Fig. 3). Since their layers have approximately equal areas and thicknesses, it means that $TiOPc_0$ is characterized by lower crystallinity. The angular positions of two most intense diffraction peaks differ insignificantly from those of $TiOPc_M$, thus quite definitely indicating that the presence/absence of magnetic field does not affect the phase composition of the resulting layers. At the same time, the ratio of diffraction peak intensities changed by 7.59° and 26.28°, thus indicating possible difference between orientations and/or quantitative ratios of the phases.

Since it was not possible to conduct reliable powder XRD analysis of TiOPc films in the standard Bragg–Brentano geometry, we measured these samples in the 2D GIXD geometry. The obtained diffraction patterns are shown in Fig. 4.

The 2D diffraction pattern of $TiOPc_M$ has separate well-localized diffraction spots and more diffuse diffraction arcs, confirming the assumption that the sample is contains two phases. In addition to the 2θ angular position, diffraction spots in the 2D picture have the azimuthal position (φ). If the azimuthal position of the central peak (corresponding to the plane of preferential orientation) is taken equal to 0°, then this value of another diffraction spot allows determining the angle between the plane of preferential orientation and the corresponding crystallographic plane [19]. In our case, this approach allows unambiguously determining the more oriented phase as modification II and assigning the following indices to the main observed reflections: (010, (020), $(\bar{1}01)$, $(1\,\bar{1}1)$, and $(\bar{1}21)$. The experimental azimuthal positions of spots $(\bar{1}01)$, $(1\,\bar{1}1)$, $(\bar{1}21)$ are equal to 71.6°, 55.4°, 30.0°, respectively, in good agreement with values 72.6°, 53.6°, 32.4° calculated from crystallographic data. Diffraction arcs of the second crystal phase are strongly diffused, which indicates lower preferential orientation and does not allow determining the azimuthal positions of the maxima with the same accuracy. Nevertheless, the comparison of angular positions of diffraction arcs with their calculated values unambiguously shows that the second crystalline phase is modification I and allows assigning indices (002), $(0\,\bar{1}1)$, $(\bar{1}11)$ to the observed diffraction arcs.

Diffraction arcs in the 2D picture of $TiOPc_0$ (Fig. 4) are much more extended, but the general view of the diffraction pattern coincides with that of $TiOPc_M$. In combination with the data obtained in the Bragg–Brentano geometry, this unambiguously shows that the presence/absence of magnetic field did not affect the phase composition of TiOPc films.

The degree of preferential orientation of a film can be estimated by measuring the azimuthal half-width of the 2D GIXD peak corresponding to the plane of preferential orientation. Fig. 5 shows the azimuthal profiles for (010) peaks of modification II in both samples and the (002) peak of modification I in the $TiOPc_M$ sample: the full width at half maximum (FWHM) of the peaks is 7.6° and 12.6°, respectively. In the case of the $TiOPc_0$ sample, the (002) reflection of modification I is too weak and diffused to build an adequate azimuth profile. Thus, the presence of magnetic field during deposition improves not only the crystallinity but also the degree of preferential orientation of crystallites. Taking into account instrumental broadening equal to ~3° (azimuthal FWHM value for the single crystal), we can conclude that the $TiOPc_M$ film has approximately twice as strong preferential orientation than the $TiOPc_0$ film. At the same time, the degree of crystallite orientation is 7 times higher in modification II than in modification I.

Information about the crystal structure of the TiOPc modification [12] and the direction of preferential orientation can be used to calculate the angles between the substrate and the molecule plane (root mean square plane passing through all C and N atoms). For the crystallites of modification II oriented along the (010) plane, this angle is equal to 62.53°. The

crystallites of modification I are oriented along the (002) plane, and the molecules are almost parallel to the substrate surface (the angle is as small as 5.30°). The arrangement of molecules relative to the substrate is shown in Fig. 7.

X-ray diffraction methods allow studying the internal structure of layers but do not provide information about their thickness and surface morphology. Therefore, we studied the samples of TiOPc layers using atomic force microscopy (AFM). Fig. 6 shows images of the surface of $TiOPc_M$ and $TiOPc_0$ sample and thickness profiles after scratching the film. As can be seen, $TiOPc_M$ consists of numerous rounded 50-150 nm grains, while the surface of $TiOPc_0$ consists of elongated conglomerates of smaller grains. The RMS roughness is approximately equal in both samples (~16 nm). The height profile shows that the thickness of both films is ~400 nm.

For comparison, the size of the coherent scattering region (CSR) can be estimated from the half-width of diffraction peaks (Fig. 3) using the the Scherrer equation. The instrumental broadening of 0.09° was determined using the LaB_6 SRM-660a reference powder sample studied under the same geometric conditions (Shimadzu XRD-7000, CuK_α radiation, Bragg–Brentano geometry). The CSR size for $TiOPc_M$ is 52 nm and 59 nm for II-triclinic and I-monoclinic phases, respectively. For the $TiOPc_0$ sample, these values are similar: 40 nm and 58 nm. Thus, the presence of magnetic field slightly increases the CSR size for modification II and has almost no effect on modification I.

To study the influence of magnetic field on sensor properties of the layers, we measured the adsorption-resistive response of $TiOPc_M$ and $TiOPc_0$ films to ammonia in the concentration range from 10 ppm to 50 ppm. The comparison of current-voltage characteristics (Fig. 8*a*) indicates that the conductivity of $TiOPc_0$ film is ~10 times lower than that of $TiOPc_M$ films. Fig. 8*b* shows that magnetic field insignificantly (1.1-1.2 times) enhanced the sensory response to ammonia, which though ranged from 0.7% to 2%. At the same time, $TiOPc_M$ layers exhibit a longer relaxation time. For the ammonia concentration of 20 ppm, the response time is 16-17 s, while the relaxation time for $TiOPc_0$ films is 60 s, and that for $TiOPc_M$

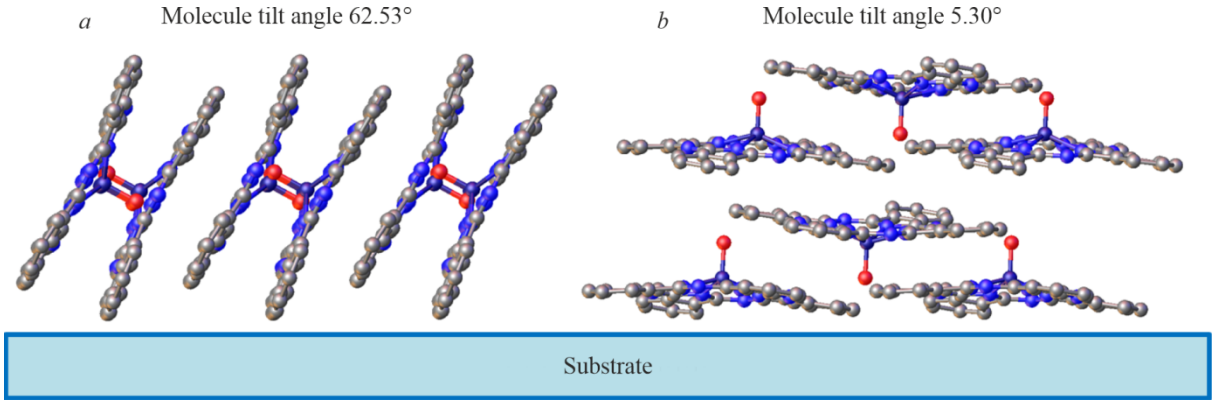

Fig. 7. Arrangement of the molecules of II-triclinic (*a*) and I-monoclinic (*b*) TiOPc modifications relative to the substrate surface.

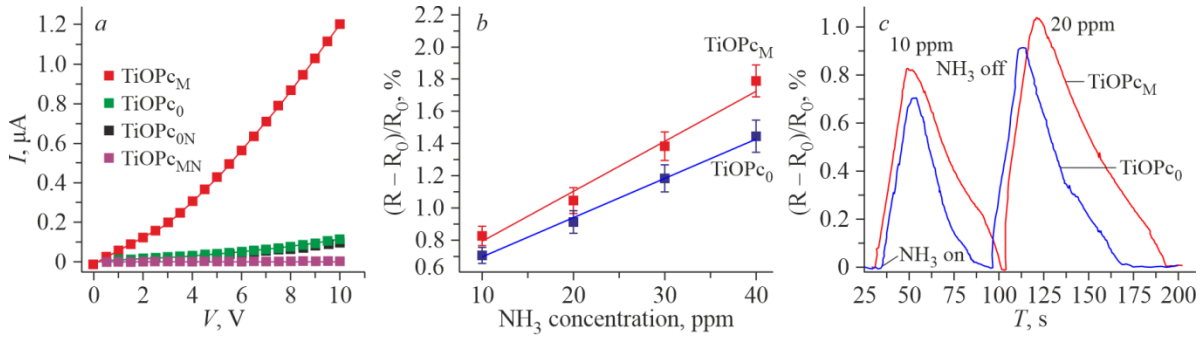

Fig. 8. Current-voltage characteristics of $TiOPc_M$ and $TiOPc_0$ layers and $TiOPc_{MN}$ and $TiOPc_{0N}$ layers irradiated by fast neutrons (*a*); sensory response of $TiOPc_M$ and $TiOPc_0$ layers as a function of ammonia concentration (*b*); typical sensory response (*c*).

films exceeds 75 s (Fig. 8*c*). In the first case (without magnetic field), irradiation of $TiOPc_0$ and $TiOPc_M$ deposited on IDE by fast neutrons with a fluence of $3 \cdot 10^{14}$ cm^{-2} on the accelerator-based neutron source of BINP SB RAS [22, 23] did not change the conductivity of the layers, while in the case of $TiOPc_M$ the conductivity decreased by two orders of magnitude (Fig. 8*a*, curves $TiOPc_{0N}$ and $TiOPc_{MN}$).

CONCLUSIONS

We investigated titanyl phthalocyanine films TiOPc deposited by vacuum thermal evaporation on glass substrates in the presence of magnetic field directed perpendicular to substrate plane and without such field. It was shown that the films in both cases consist of two polymorphs (II-triclinic and I-monoclinic) and have a strong preferential orientation. Magnetic field does not affect the phase composition of the films but significantly increases their crystallinity and the orientation degree. The AFM results showed that the magnetic field slight increases the size of individual grains, while the total thickness of the films and their roughness remain the same. The main positive effect of magnetic field is markedly increased conductivity of the obtained layers. The sensory response to ammonia and the relaxation time increase insignificantly.

FUNDING

This work was funded by the Ministry of Science and Higher Education of the Russian Federation: project No. 121031700314-5 (synthesis, film deposition, study of sensory properties); project No. 121031700313-8 and "Priority 2030" program (XRD and crystal chemical studies).

CONFLICT OF INTERESTS

The authors declare that they have no conflicts of interests.

REFERENCES

1. C. Wang, H. Dong, W. Hu, Y. Liu, and D. Zhu. Semiconducting π-conjugated systems in field-effect transistors: A material odyssey of organic electronics. *Chem*. *Rev*., **2012**, *112*(4), 2208-2267. https://doi.org/10.1021/cr100380z
2. D. Mukherjee, R. Manjunatha, S. Sampath, and A. K. Ray. Phthalocyanines as Sensitive Materials for Chemical Sensors. In: Materials for Chemical Sensing. Cham: Springer International Publishing, **2017**, 165-226. https://doi.org/10.1007/978-3-319-47835-7_8
3. Y.-L. Lee, W.-C. Tsai, and J.-R. Maa. Effects of substrate temperature on the film characteristics and gas-sensing properties of copper phthalocyanine films. *Appl*. *Surf*. *Sci*., **2001**, *173*(3/4), 352-361. https://doi.org/10.1016/s0169-4332(01)00019-8
4. K. Xiao, Y. Liu, G. Yu, and D. Zhu. Influence of the substrate temperature during deposition on film characteristics of copper phthalocyanine and field-effect transistor properties. *Appl*. *Phys*., *A*, **2003**, *77*(3/4), 367-370. https://doi.org/10.1007/s00339-003-2169-6
5. C. Schünemann, C. Elschner, A. A. Levin, M. Levichkova, K. Leo, and M. Riede. Zinc phthalocyanine - Influence of substrate temperature, film thickness, and kind of substrate on the morphology. *Thin Solid Films*, **2011**, *519*(11), 3939-3945. https://doi.org/10.1016/j.tsf.2011.01.356
6. S. Zhu, C. E. Banks, D. O. Frazier, B. Penn, H. Abdeldayem, R. Hicks, H. D. Burns, and G. W. Thompson. Structure and morphology of phthalocyanine films grown in electrical fields by vapor deposition. *J*. *Cryst*. *Growth*, **2000**, *211*(1-4), 308-312. https://doi.org/10.1016/s0022-0248(99)00773-3

7. B.-E. Schuster, T. V. Basova, H. Peisert, and T. Chassé. Electric field assisted effects on molecular orientation and surface morphology of thin titanyl(IV)phthalocyanine films. *ChemPhysChem*, **2009**, *10*(11), 1874-1881. https://doi.org/10.1002/cphc.200900087
8. W. Hu. Highly ordered vacuum-deposited thin films of copper phthalocyanine induced by electric field. *Thin Solid Films*, **1999**, *347*(1/2), 299-301. https://doi.org/10.1016/s0040-6090(99)00010-3
9. Z. G. Ji, K. W. Wong, P. K. Tse, R. W. M. Kwok, and W. M. Lau. Copper phthalocyanine film grown by vacuum deposition under magnetic field. *Thin Solid Films*, **2002**, *402*(1/2), 79-82. https://doi.org/10.1016/s0040-6090(01)01702-3
10. V. Kolotovska, M. Friedrich, D. R. T. Zahn, and G. Salvan. Magnetic field influence on the molecular alignment of vanadyl phthalocyanine thin films. *J. Cryst. Growth*, **2006**, *291*(1), 166-174. https://doi.org/10.1016/j.jcrysgro.2006.02.016
11. A. Hoshino, Y. Takenaka, and H. Miyaji. Redetermination of the crystal structure of α-copper phthalocyanine grown on KCl. *Acta Crystallogr., Sect. B: Struct. Sci.*, **2003**, *59*(3), 393-403. https://doi.org/10.1107/s010876810300942x
12. W. Hiller, J. Strähle, W. Kobel, and M. Hanack. Polymorphie, Leitfähigkeit und Kristallstrukturen von Oxo-phthalocyaninato-titan(IV). *Z. Kristallogr. – Cryst. Mater.*, **1982**, *159*(1-4), 173-184. https://doi.org/10.1524/zkri.1982.159.14.173
13. K. Oka, O. O. Okimasa Okada, and K. N. Katumi Nukada. Study of the crystal structure of titanylphthalocyanine by Rietveld analysis and intermolecular energy minimization method. *Jpn. J. Appl. Phys.*, **1992**, *31*(7R), 2181. https://doi.org/10.1143/jjap.31.2181
14. T. Bluhm. The application of Rietveld analysis to crystal structures of titanyl phthalocyanine. *Proc. SPIE*, **1992**, *1670*, 16. https://doi.org/10.1117/12.2322225
15. O. Okada, K. O. Kozo Oka, and M. I. Masakazu Iijima. Study of the crystal structure of titanylphthalocyanine by Rietveld analysis. II. *Jpn. J. Appl. Phys.*, **1993**, *32*(8R), 3556. https://doi.org/10.1143/jjap.32.3556
16. B.-A. Paez-Sierra, V. Kolotovska, V.-T. Rangel-Kuoppa, J. Ihm, and H. Cheong. Engineered molecular layers for organic electronic applications: A confocal scanning raman spectroscopy (CSRS) investigation. **2011**, 873-874. https://doi.org/10.1063/1.3666654
17. B. A. Paez-Sierra, F. Mesa, and A. Dussan. Raman analysis of vanadyl phthalocynine layers for plastic electronic applications. *Appl. Mech. Mater.*, **2015**, *789*/*790*, 170-175. https://doi.org/10.4028/www.scientific.net/amm.789-790.170
18. M. Atzori, L. Tesi, E. Morra, M. Chiesa, L. Sorace, and R. Sessoli. Room-temperature quantum coherence and Rabi oscillations in vanadyl phthalocyanine: Toward multifunctional molecular spin qubits. *J. Am. Chem. Soc.*, **2016**, *138*(7), 2154-2157. https://doi.org/10.1021/jacs.5b13408
19. A. S. Sukhikh, T. V. Basova, and S. A. Gromilov. The use of 2D diffractometry data for oriented samples in the choice of a unit cell. *J. Struct. Chem.*, **2017**, *58*(5), 953-963. https://doi.org/10.1134/s0022476617050146
20. A. B. Rodriguez-Navarro. XRD2DScan: new software for polycrystalline materials characterization using two-dimensional X-ray diffraction. *J. Appl. Crystallogr.*, **2006**, *39*(6), 905-909. https://doi.org/10.1107/s0021889806042488
21. D. Nečas and P. Klapetek. Gwyddion: an open-source software for SPM data analysis. *Open Phys.*, **2012**, *10*(1). https://doi.org/10.2478/s11534-011-0096-2
22. S. Taskaev, E. Berendeev, M. Bikchurina, T. Bykov, D. Kasatov, I. Kolesnikov, A. Koshkarev, A. Makarov, G. Ostreinov, V. Porosev, S. Savinov, I. Shchudlo, E. Sokolova, I. Sorokin, T. Sycheva, and G. Verkhovod. Neutron Source Based on Vacuum Insulated Tandem Accelerator and Lithium Target. *Biology*, **2021**, *10*(5), 350. https://doi.org/10.3390/biology10050350
23. D. A. Kasatov, A. M. Koshkarev, A. N. Makarov, G. M. Ostreinov, S. Y. Taskaev, and I. M. Shchudlo. A fast-neutron source based on a vacuum-insulated tandem accelerator and a lithium target. *Instrum. Exp. Tech.*, **2020**, *63*(5), 611-615. https://doi.org/10.1134/s0020441220050152